

## PREPARATION OF Fe-Si-B-(Cu,Nb,Ni,Mo) FILMS BY QUENCHING FROM A VAPOR STATE

S. I. Ryabtsev<sup>1\*</sup>, O. I. Kushnerov<sup>1</sup>, V. F. Bashev<sup>2</sup>, T. V. Kalinina<sup>2</sup>, T. M. Dorozhka<sup>2</sup>

<sup>1</sup>*Oles Honchar Dnipro National University, Dnipro, Ukraine*

<sup>2</sup>*Dnipro State Technical University, Kamianske, Dnipropetrovsk region, Ukraine*

\**e-mail: siryabts@gmail.com*

Using modernized three-electrode ion-plasma sputtering, homogeneous thin films of Fe-Si-B-(Cu, Nb), and Fe-Si-B-(Ni, Mo) were obtained. The structure of the films was investigated by X-ray diffraction and electron microscopy. It was established that as a result of sputtering, amorphous and nanocrystalline phases with a coherent scattering region (CSR) size of 1.6 nm and 12 nm were formed in the Fe<sub>73</sub>Si<sub>16</sub>B<sub>7</sub>-(Cu, Nb)<sub>4</sub> and Fe<sub>78.5</sub>Si<sub>6</sub>B<sub>14</sub>-(Ni, Mo)<sub>1.5</sub> films. The thermal stability of metastable states of the films, as well as the electrical and magnetic properties of freshly prepared and heat-treated films were studied. The conditions for obtaining films with small (modulo) values of the temperature coefficient of electrical resistance ( $-0.9 \cdot 10^{-5} \text{ K}^{-1}$ ) and coercive force ( $H_C \sim 11 \text{ A/m}$ ) were determined.

**Keywords:** thin film, ion-plasma sputtering, amorphous structure, coercive force, metastable state, temperature coefficient of resistance.

Received 06.11.2023; Received in revised form 08.12.2023; Accepted 15.12.2023

### 1. Introduction

One of the main tasks is the creation of new materials with high functional characteristics and methods for their production. The development of current information, nano- and biotechnologies depends on its solution. In recent decades, researchers have paid much attention to materials with an extremely nonequilibrium amorphous structure [1-2]. Modern methods of quenching from a liquid or vapor state, such as laser processing, electrochemical deposition, three-electrode ion plasma sputtering, extreme plastic deformation [3-7], have significantly increased the number of substances obtained in a non-crystalline state. The study of the physical properties of thin metal films has been stimulated by using metal condensates in microelectronics and microwave technology. The transition from bulk materials to films makes it possible to place up to 100 million elements in  $1 \text{ cm}^3$ . By improving the production methods of such materials and changing the deposition conditions (substrate temperature, flux density, composition of residual gases), it is possible to purposefully influence the structure of films in a very wide range [9, 10]. The structural characteristics of thin films are closely related to the kinetics of condensate formation and secondary processes occurring during and after deposition [11]. Therefore, the development and research of new film structures obtained by improved deposition methods is very important. Of particular interest are multicomponent films based on the Fe-Si-B system, which have excellent soft magnetic properties.

### 2. Experimental procedure

The method of modernized three-electrode ion-plasma sputtering (TIPS) [12] was used to deposit the films. For this method, at an accelerating voltage of 2 kV, it is theoretically predicted that the kinetic energy of the deposited atoms changes from 100 to 200 eV by lowering the pressure of the plasma-generating gas from 0.053 to 0.016 Pa [13]. Moreover, this method demonstrated the ability to produce uniform films of immiscible binary metal systems [10, 12]. The targets for film deposition were rapidly cooled ribbons of the same composition, obtained by quenching from a liquid state. The sputtered targets were parallelepipeds  $0.02 \times 0.02 \text{ m}$  in size and 0.02 mm high. The targets were in 16 cells, the walls of which acted as electrostatic lenses. As a result, compared with the conventional three-electrode ion-plasma sputtering, the energy of the sputtered atoms before the collision

with the substrate increases by a factor of 5–7. The relaxation rate of atom's energy under such deposition modes is theoretically estimated at  $10^{12}$ – $10^{14}$  K/s [14], which is 7–8 orders of magnitude higher than the maximum cooling rates achieved during fast quenching of metals from a liquid state. This allows us to talk about ultrafast quenching from a vapor state.

The films were deposited simultaneously on glass-ceramic (sital) substrates and on fresh cleavages of a NaCl single monocrystals. The thickness was calculated from the measured mass of the film and varied from 153 to 175 nm depending on the mode, composition, and time of application. The deposition conditions are given in Table 1.

Table 1

**The method of modernized three-electrode ion-plasma sputtering for film production and its parameters**

Sample number, film composition (at. %)	$U_T$ , kV	$I_A$ , A	$P$ , mPa	$v$ , nm/s	$d$ , nm	$t$ , min
1, Fe+16%Si+7%B+1%Cu+3%Nb	2	0.8	17	0,16	153	16
2, Fe+6%Si+14%B+1%Ni+0,5%Mo	2	0.8	18	0,18	176	16

Note:  $U_T$  – accelerating voltage applied to the target;  $I_A$  – plasma discharge current;  $P$  – plasma gas pressure;  $v$  – the film thickness growth rate;  $d$  – the film thickness;  $t$  – deposition time.

The structure of films deposited on single-crystal NaCl substrates was studied by transmission electron microscopy and X-ray diffraction analysis in filtered cobalt  $K_\alpha$  radiation after dissolving the salt. The physical properties of nonequilibrium states were studied on films deposited on glass-ceramic substrates. The electrical resistance of films was measured by four probe method in a vacuum of  $\sim 10$  mPa during continuous heating and cooling of the sample at a rate from 4 to 18 K/min to study the electrical properties and thermal stability of films. The magnetic properties of the samples were measured by a vibrating sample magnetometer in a magnetic field with a maximum induction of 0.3 T, parallel to the film plane, at room temperature.

The multicomponent films of composition (in at. %):  $Fe_{73}Si_{16}B_7-(Cu, Nb)_4$  (composition 1) and  $Fe_{78,5}Si_6B_{14}-(Ni, Mo)_{1,5}$  (composition 2) were the subject of this investigation.

### 3. Results and discussion

In the films of composition 1 in the newly deposited state, an amorphous structure with a fuzzy halo was observed, indicating a CSR size of approximately 1.6 nm (Fig. 1).

In the films of composition 2, a nanocrystalline structure was established with a CSR size of  $L \approx 12$  nm (Fig. 2). These CSR sizes roughly match the grain sizes, which allows us to categorize the structure as nanocrystalline [15]. The temperatures of the start and end of the decay of the arising metastable states are estimated based on the points on the temperature dependence, where the irreversible drop in electrical resistance starts (Fig. 3). The structure of the films (composition 1) shows stability up to the temperature of 773 K. For these films, the temperature coefficient of resistance is  $-21 \cdot 10^{-5} K^{-1}$ . Films of composition 2 are stable up to 703 K and have the temperature coefficient of resistance  $-0.9 \cdot 10^{-5} K^{-1}$ . At 773 K for composition 1 and 703 K for composition 2, the onset of the decay of metastable structures is seen with the emergence of a supersaturated solid solution of  $\alpha$ -Fe (Fig. 1, 2).

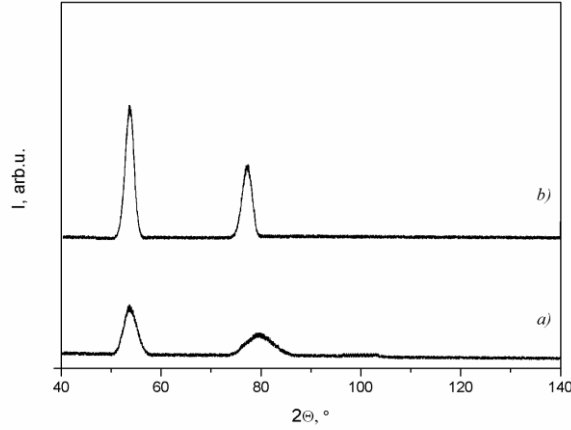


**Fig. 1. Photometric X-ray diffraction profiles of the films: (a)  $\text{Fe}_{78.5}\text{Si}_6\text{B}_{14}\text{-(Ni, Mo)}_{1.5}$  (composition 1); (b)  $\text{Fe}_{78.5}\text{Si}_6\text{B}_{14}\text{-(Ni, Mo)}_{1.5}$  (composition 2) in the initial state.**

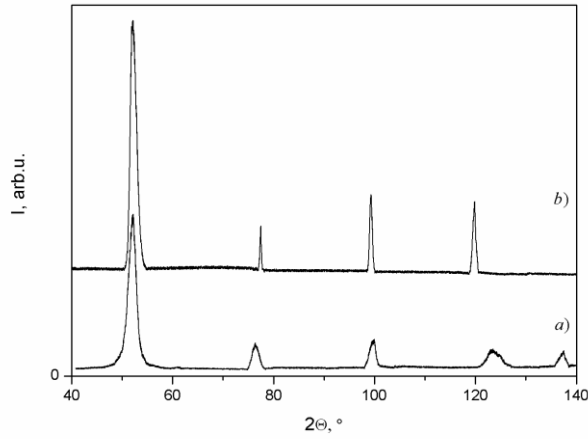


**Fig. 2. Photometric X-ray diffraction profiles of the films: (a)  $\text{Fe}_{78.5}\text{Si}_6\text{B}_{14}\text{-(Ni, Mo)}_{1.5}$  (composition 1); (b)  $\text{Fe}_{78.5}\text{Si}_6\text{B}_{14}\text{-(Ni, Mo)}_{1.5}$  (composition 2) after heating to 893 K (b).**

The temperature dependence (Fig. 3) of reaching the maximum value of the relative change in electrical resistance ( $R/R_0$ ) was used to estimate the activation energy of the relaxation processes of the initial metastable structures, if the same degree of relaxation of the structure corresponds to the maximum values of  $R/R_0$  for a single-phase interval, obtained at different heating rates ( $V_{\text{heat}}$ ). In this case, the parameter  $\tau_{\text{max}} = (T_{\text{decomp}}^2 / V_{\text{heat}})$  follows an Arrhenius-type equation and describes the kinetics of this process, (here  $T_{\text{decomp}}$  is the temperature at which the metastable structure starts to decompose). The activation energy values are determined based on the slope of  $\ln(\tau_{\text{max}})$  to the axis ( $1000/T_{\text{decomp}}$ ) for different rates of cooling.

The activation energy values obtained by the Kissinger method are  $10400 \pm 1200$  K. This value is four times lower than the activation energy values (43000 K) and the average diffusion coefficient determined from the kinetic parameters in the  $\text{Fe}_{40}\text{Ni}_{40}\text{P}_{14}\text{B}_6$  alloy quenched from the liquid state [16].

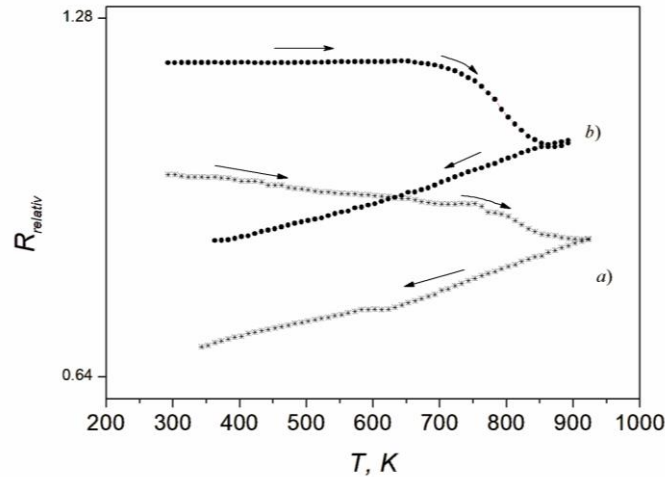


Fig. 3. The resistivity of the films of composition 1 (a) and composition 2 (b) as a function of temperature.

The literature has already reported such a difference between the activation energies for films and bulk samples. This can be attributed to the near two-dimensionality of the films studied compared to foils quenched from the liquid state and geometric factors.

The demagnetizing magnetic field strength ( $H_C$ ) of newly deposited films of compositions 1 and 2 (Fig. 4) is twice as large as the  $H_C$  of films of pure iron and equals to 11 and 10 A/m, respectively. After heating the films of composition 1 to 893 K,  $H_C$  rises by 1.1 times, and in films of composition it rises 2 by 1.2 times, which is due to the formation of the optimal ratio between particles of nanocrystalline  $\alpha$ -Fe and amorphous phase remnants.

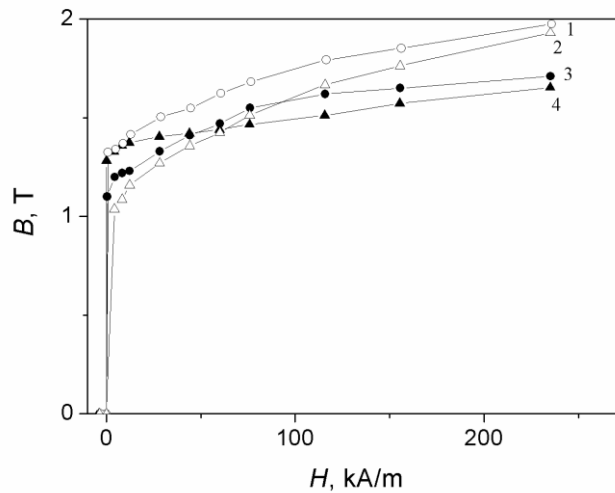


Fig. 4. Demagnetization plots for films aligned parallel to the field: 1 – initial state of composition 2; 2 – composition 2 after heating to 893 K; 3 – initial state of composition 1; 4 – composition 1 after heating to 893 K.

#### 4. Conclusions

The structure and properties of  $\text{Fe}_{73}\text{Si}_{16}\text{B}_7\text{-(Cu, Nb)}_4$  and  $\text{Fe}_{78.5}\text{Si}_6\text{B}_{14}\text{-(Ni, Mo)}_{1.5}$  films produced by modernized three-electrode ion-plasma sputtering were studied under heating. It was found that sputtering  $\text{Fe}_{73}\text{Si}_{16}\text{B}_7\text{-(Cu, Nb)}_4$  alloy results in an amorphous phase with a coherent scattering region size of 1.6 nm in the films. Sputtering  $\text{Fe}_{78.5}\text{Si}_6\text{B}_{14}\text{-(Ni, Mo)}_{1.5}$  alloy leads to a nanocrystalline phase with a coherent scattering region size of 12 nm in the films. The emerging metastable structures are stable when heated to 773 K in  $\text{Fe}_{73}\text{Si}_{16}\text{B}_7\text{-(Cu, Nb)}_4$  films and to 703 K in  $\text{Fe}_{78.5}\text{Si}_6\text{B}_{14}\text{-(Ni, Mo)}_{1.5}$  films. The activation energy of relaxation processes of the initial metastable structures was estimated based on the temperature dependences of electrical resistance at different heating rates. The activation energy values obtained by the Kissinger method are  $10400 \pm 1200$  K. It is demonstrated that films of the composition  $\text{Fe}_{78.5}\text{Si}_6\text{B}_{14}\text{-(Ni, Mo)}_{1.5}$  have a low temperature coefficient of resistance  $-0.9 \cdot 10^{-5} \text{ K}^{-1}$ . It was revealed that the coercive force of newly deposited films is 10–11 A/m, which is more than twice the coercive force of films of pure iron and ribbons of a similar composition quenched from a liquid state. These differences in physical properties can be attributed to geometric factors (two-dimensionality of the sample) and the structure element sizes.

#### References

1. **Yan, L.** Fabrication of Fe-Si-B Based Amorphous Powder Cores by Spark Plasma Sintered and Their Magnetic Properties. / L. Yan, B. Yan, Y. Jian // *Materials*. – 2022. – Vol. 15, Issue 4. – P. 1603 – 1615. doi: 10.3390/ma15041603
2. **Dong, Y.** The effects of field annealing on the magnetic properties of FeSiB amorphous powder cores / Y. Dong, Z. Li, M. Liu et al. // *Materials Research Bulletin*. – 2017. – Vol. 96, Part 3. – P. 160 – 163. doi: 10.1016/j.materresbull.2017.04.030
3. **Girzhon, V. V.** Analysis of structure formation processes features in high-entropy alloys of Al-Co-Cr-Fe-Ni system during laser alloying / V.V. Girzhon, V. V. Yemelianchenko, O. V. Smolyakov et al. // *Results Mater.* – 2022. – Vol 15. – P. 100311 – 100316. doi: 10.1016/j.rinma.2022.100311
4. **Jia, X.** Effects of Si content on structure and soft magnetic properties of  $\text{Fe}_{81.3}\text{Si}_x\text{B}_{17-x}\text{Cu}_{1.7}$  nanocrystalline with pre-existing  $\alpha$ -Fe nanocrystals / X. Jia, W. Zhang, Y. Dong et al. // *J. Mater Sci.* – 2021. – Vol. 56. – P. 2539 – 2548. doi: 10.1007/s10853-020-05404-w
5. **Lashgari, H. R.** Thermal stability, dynamic mechanical analysis and nanoindentation behavior of FeSiB(Cu) amorphous alloys / H. R. Lashgari, Z. Chen, X. Z. Liao et al. // *Materials Science & Engineering A*. – 2015. – Vol. 626. – P. 480 – 499. doi: 10.1016/j.msea.2014.12.097
6. **Han, Y.** New Fe-based soft magnetic amorphous alloys with high saturation magnetization and good corrosion resistance for dust core application / Y. Han, F. L. Kong, F. F. Han et al. // *Intermetallics*. – 2016. – Vol. 76. – P. 18 – 25. doi: 10.1016/j.intermet.2016.05.011
7. **Neamtu, B. V.** Preparation and soft magnetic properties of spark plasma sintered compacts based on Fe–Si–B glassy powder / B. V. Neamtu, T. F. Marinca, I. Chicinaş et al. // *Journal of Alloys and Compounds*. – 2014. – Vol. 600. – P. 1 – 7. doi: 10.1016/j.jallcom.2014.02.115
8. **Kuji, Ch.** Relationship between blanking performance and microstructure of annealed Fe–Si–B–Cr amorphous alloy sheets. / Ch. Kuji, M. Mizutani, K. Takenaka et al. // *Precision Engineering*. – 2023. – Vol. 82. – P. 33 – 43. doi: 10.1016/j.precisioneng.2023.03.004

9. **Dotsenko, F. F.** Emission properties of thin-film alloys of immiscible components / F. F. Dotsenko, V. F. Bashev, S. I. Ryabtsev et al. // *Phys. Met. Metallogr.* – 2010. – Vol. 110, No. 3. – P. 223 – 228. doi:10.1134/S0031918X1009005X
10. **Bashev, V.** Films of immiscible systems obtained by three-electrode ion-plasma sputtering / V. Bashev, O. Kushnerov, N. Kutseva et al. // *Mol. Cryst. Liq. Cryst.* – 2021. – Vol. 721, No. 1. – P. 30 – 37. doi:10.1080/15421406.2021.1905274
11. **Bashev, V. F.** Electrical properties and structure of W-Ba films in fresh-sputtered and equilibrated states / V. F. Bashev, F. F. Dotsenko, S. I. Ryabtsev // *Phys. Met. Metallogr.* – 1995. – Vol. 80, No. 1. – P. 79 – 82.
12. **Bashev, V. F.** Effect of nonequilibrium vapor deposition on phase composition and properties of Fe-Mg films / V. F. Bashev, O. E. Beletskaya, Z. V. Balyuk et al. // *Phys. Met. Metallogr.* – 2003. – Vol. 96, No. 1. – P. 72 – 74.
13. **Dotsenko, F. F.** Fizychni peredumovy formuvannya nadnerivnovazhnykh staniv ta otsinka skladu napylenykh splaviv / F. F. Dotsenko, V. F. Bashev // *Visnyk Dnipropetrovskoho Universytetu. Fizyka. Radioelektronika.* – 2001. – Vol. 7. – P. 8 – 17.
14. **Grant, U. A.** Preparation of amorphous alloys using ion implantation / U. A. Grant, A. Ali, L. T. Chadderton et al. // *Fast-Quenched Metals* / Editor B. Cantor. – Moscow: Metallurgiya 1983. – P. 52 – 57.
15. **Ungár, T.** Correlation between subgrains and coherently scattering domains / T. Ungár, G. Tichy, J. Gubicza, R. J. Hellmig // *Powder Diffraction.* – 2005. – Vol. 20, Issue 4. – P. 366 – 375. doi: 10.1154/1.2135313
16. **Tkach, V. I.** Relaxation kinetics of metallic glass  $\text{Fe}_{40}\text{Ni}_{40}\text{P}_{14}\text{B}_6$  under isothermal conditions. / V. I. Tkach, A. I. Limanovsky, S. N. Denisenko, O. N. Beloshov // *Izvestiya RAN. Seriya fizicheskaya.* – 1997. – Vol. 61, No. 2. – P. 221 – 227.